ISSN 1063-7834, Physics of the Solid State, 2020, Vol. 62, No. 2, pp. 285–290. © Pleiades Publishing, Ltd., 2020.
Russian Text © The Author(s), 2020, published in Fizika Tverdogo Tela, 2020, Vol. 62, No. 2, pp. 235–240.

MAGNETISM

Synthesis and Magnetic Properties of the Core–Shell $Fe_3O_4/CoFe_2O_4$ Nanoparticles

D. A. Balaev[a, *], S. V. Semenov[a], A. A. Dubrovskii[a], A. A. Krasikov[a], S. I. Popkov[a], S. S. Yakushkin[b], V. L. Kirillov[b], and O. N. Mart'yanov[b]

[a] *Kirensky Institute of Physics, Krasnoyarsk Scientific Center, Siberian Branch, Russian Academy of Sciences, Krasnoyarsk, 660036 Russia*

[b] *Boreskov Institute of Catalysis, Siberian Branch, Russian Academy of Sciences, Novosibirsk, 630090 Russia*

**e-mail: dabalaev@iph.krasn.ru*

Received September 16, 2019; revised September 16, 2019; accepted September 16, 2019

Abstract—The $Fe_3O_4/CoFe_2O_4$ nanoparticles with a core–shell structure with an average size of 5 nm have been obtained by codeposition from the iron and cobalt chloride solutions. An analysis of the magnetic properties of the obtained system and their comparison with the data for single-phase Fe_3O_4 (4 nm) and $CoFe_2O_4$ (6 nm) nanoparticles has led to the conclusion about a noticeable interaction between the soft magnetic (Fe_3O_4) and hard magnetic ($CoFe_2O_4$) phases forming the core and shell of hybrid particles.

Keywords: oxide nanoparticles, core–shell structure, coercivity

DOI: 10.1134/S1063783420020043

1. INTRODUCTION

Magnetic nanoparticles with a pronounced core/shell structure are widely used in medicine, catalysis, including targeted drug delivery systems [1], magnetically separable catalysts [2, 3], magnetic hyperthermia [4], magnetic memory, and spintronics [5]. The magnetic properties of nanostructured systems are determined not only by the molecular formula of components, but also by the presence of nanoscale inhomogeneities [5]. The high sensitivity of magnetic interactions to structural inhomogeneities is a key factor that opens great opportunities for creating systems with unique properties [6–8], which evokes increased interest of researchers.

A way of improving the magnetic characteristics of nanoparticles is the creation of core–shell systems consisting of a soft magnetic material with the low coercivity and a hard magnetic material with the higher coercivity. The magnetic and exchange interactions inside an individual nanoparticle, along with the interparticle interactions, are of great importance for the formation of macroscopic properties of the entire magnetic system, as well as for the effective interaction of its individual particles with an ac electromagnetic field. Within this paradigm, MFe_2O_4 (M = Fe, Co, Mn) particles and core–shell ferrite nanoparticles consisting of a hard magnetic core ($CoFe_2O_4$) and a magnetite shell (Fe_3O_4) have recently been studied to check the efficiency of their use in hyperthermia [9–15]. The magnetic measurements show that the coating of the $CoFe_2O_4$ hard magnetic phase with magnetite ensures a fairly high coercivity and thereby enhances the efficiency of magnetic hyperthermia. At the same time, the biologically safe outer shell of magnetite makes such systems attractive for medical applications.

The core–shell nanoparticles with an inverse composition, i.e., with the Fe_3O_4 core and $CoFe_2O_4$ shell, have been studied less intensively [16, 17]. Meanwhile, such hybrid particles are not only promising for biomedical applications, but also are an excellent model system for studying nanomagnetism and magnetic exchange coupling. Indeed, the interaction of spins at the interface between different magnetic phases leads, for example, to the exchange bias or exchange spring effect [18]. These phenomena are often united by the term 'magnetic hysteresis loop tailoring,' when a careful selection of the parameters of a complex magnetic system provides tunable dynamic magnetic properties [19]. An example was given in [20], where the authors managed to obtain particles with a high response to an external magnetic field and, at the same time, zero residual magnetization, which is of crucial importance for use in cancer treatment.

In real dispersed systems based on the core–shell nanoparticles, the resulting magnetic response will be determined by the interaction of spins of the interface between two phases [5, 21] and magnetic interparticle interactions [22] with regard to the superparamagnetic behavior of individual (isolated) nanoparticles. In

view of this, it is important to obtain nanoparticles with a specified size distribution and high uniformity. In this case, the synthesized particles must be really core–shell rather than a mixture of nanoparticles of two types. Recently, we proposed a new method for synthesizing ultrafine (4 nm) magnetite nanoparticles by codeposition in a mixed water–dimethyl sulfoxide (DMSO) solvent [23, 24]. In this study, the method was modified for obtaining the core-shell Fe_3O_4–$CoFe_2O_4$ nanoparticles. The aim of the first stage of this work was to obtain magnetite particles with a characteristic size of 4–6 nm and a $CoFe_2O_4$ surface layer thickness of about 1 nm and investigate their structural and magnetic properties. For the correct comparison of the obtained data, reference samples of Fe_3O_4 and $CoFe_2O_4$ nanoparticles with similar sizes were examined.

2. EXPERIMENTAL

The nanoparticles under study were synthesized by codeposition from the iron and cobalt chloride solutions.

The reference samples of magnetite particles (hereinafter referred to as sample *S*1) and cobalt ferrite (hereinafter referred to as sample *S*3) were synthesized by codeposition with propylene oxide (PO) from a solution of crystalline hydrates of iron(II) and (III) chlorides ($Fe^{3+}/Fe^{2+} = 2$) in DMSO ($[Fe^{3+} + Fe^{2+}] =$ 0.115 mol/L and PO/Cl = 2.215) in an inert atmosphere and from a solution of crystalline hydrates of iron(III) and cobalt(II) chlorides ($Fe^{3+}/Co^{2+} =$ 2(1.998) in ethanol rectificate (93.2%) (at $[Fe^{3+} +$ $Co^{2+}] = 0.334$ mol/L and PO/Cl = 4.6), respectively.

The core–shell particles (hereinafter referred to as sample *S*2) were synthesized by codeposition from an aqueous solution of iron(III) and (II) and cobalt(II) chlorides ($Fe^{3+}/(Fe^{2+} + Co^{2+}) = 2$) with a 20% aqueous solution of NH_3 ($[Fe^{3+} + Fe^{2+} + Co^{2+}] =$ 0.15 mol/L, pH = 9.5). At the used ratio $Co^{2+}/Fe^{2+} =$ 7, the magnetite core in the forming particles is twice as small as their total size. In contrast to ferrite, the magnetite phase is formed at room temperature; consequently, this phase forms the central part (core) of a particle. To complete the formation of the ferrite shell, a sealed mixture was exposed at 70°C for 2 h.

High resolution transmission electron microscopy (HRTEM) images were obtained on a JEOL JEM-2010 microscope at an accelerating voltage of 200 kV with a resolution of 1.4 Å.

The magnetic properties were measured on a vibrating sample magnetometer [25] and a PPMS-6000 Physical Property Measurement System at the Center for Collective Use, Krasnoyarsk Scientific Center, Siberian Branch, Russian Academy of Sciences.

Table 1. Ratio between Fe_3O_4 and $CoFe_2O_4$ in the nanoparticle samples, HRTEM average size, and calculated cobalt ferrite spacer thickness t_{shell}

Sample	Fe_3O_4, vol %	$CoFe_2O_4$, vol %	d, nm	d_{core}, nm	t_{shell}, nm
*S*1 (Fe_3O_4)	100	0	~3.9	–	–
*S*2 (1 : 7)	12.5	87.5	~5.0	~2.5	~1.25
*S*3 ($CoFe_2O_4$)	0	100	~6.0	–	–

3. RESULTS AND DISCUSSION

Figure 1 shows HRTEM micrographs of particles of the investigated samples. It can be seen that most particles in the investigated samples are smaller than 10 nm. The particle size distribution histograms obtained using a representative array of microphotographs confirm this conclusion (Fig. 1). Table 1 gives the average particle sizes obtained using the HRTEM data, volume ratio of Fe_3O_4 and $CoFe_2O_4$ from the synthesis conditions, and, for $Fe_3O_4/CoFe_2O_4$ (sample *S*2), the calculated cobalt ferrite layer thickness t_{shell}. The interplanar spacings determined using the HRTEM method correspond to a spinel ferrite structure. At the same time, the difference between the Fe_3O_4 and $CoFe_2O_4$ lattice parameters is minor and, in sample *S*2, the $CoFe_2O_4$ shell cannot be distinguished from the Fe_3O_4 core in the HRTEM data. To prove sample *S*2 to be not a mixture of Fe_3O_4 and $CoFe_2O_4$ nanoparticles, it is necessary to compare the magnetic properties of a series of such samples.

Figure 2 shows temperature dependences of magnetization $M(T)$ for the investigated samples in a field of $H = 1$ kOe. The dependences were measured in the zero field cooling (ZFC) and field cooling (FC, $H =$ 1 kOe) modes. All the dependences are typical of superparamagnetic (SP) systems: there is a distinct maximum in the $M(T)_{ZFC}$ dependence (at temperature T_{max}) and reversible magnetization (no thermomagnetic prehistory effect) at temperatures slightly higher than T_{max}. The T_{max} values in a field of $H = 1$ kOe are about 26, 160, and 296 K for samples *S*1, *S*2, and *S*3, respectively. It should be noted that, in the general case, the temperature T_{max} does not coincide with the temperature T_B of the superparamagnetic blocking of medium-size particles [26, 27]. The average blocking temperature $\langle T_B \rangle$ is defined as a maximum of the derivative $d\{M(T)_{ZFC} - M(T)_{FC}\}/dT$ [26–29]. The $\langle T_B \rangle$ values obtained in the described way are about 60 and 190 K for samples *S*2 and *S*3, respectively.

We would like to note an important fact that, for sample *S*2, the only distinct maximum is observed in the $M(T)_{ZFC}$ dependence. This indirectly indicates that the particles in sample *S*2 manifest themselves in the magnetic measurements as a single system. Indeed, the magnetite particle size in sample *S*1 is

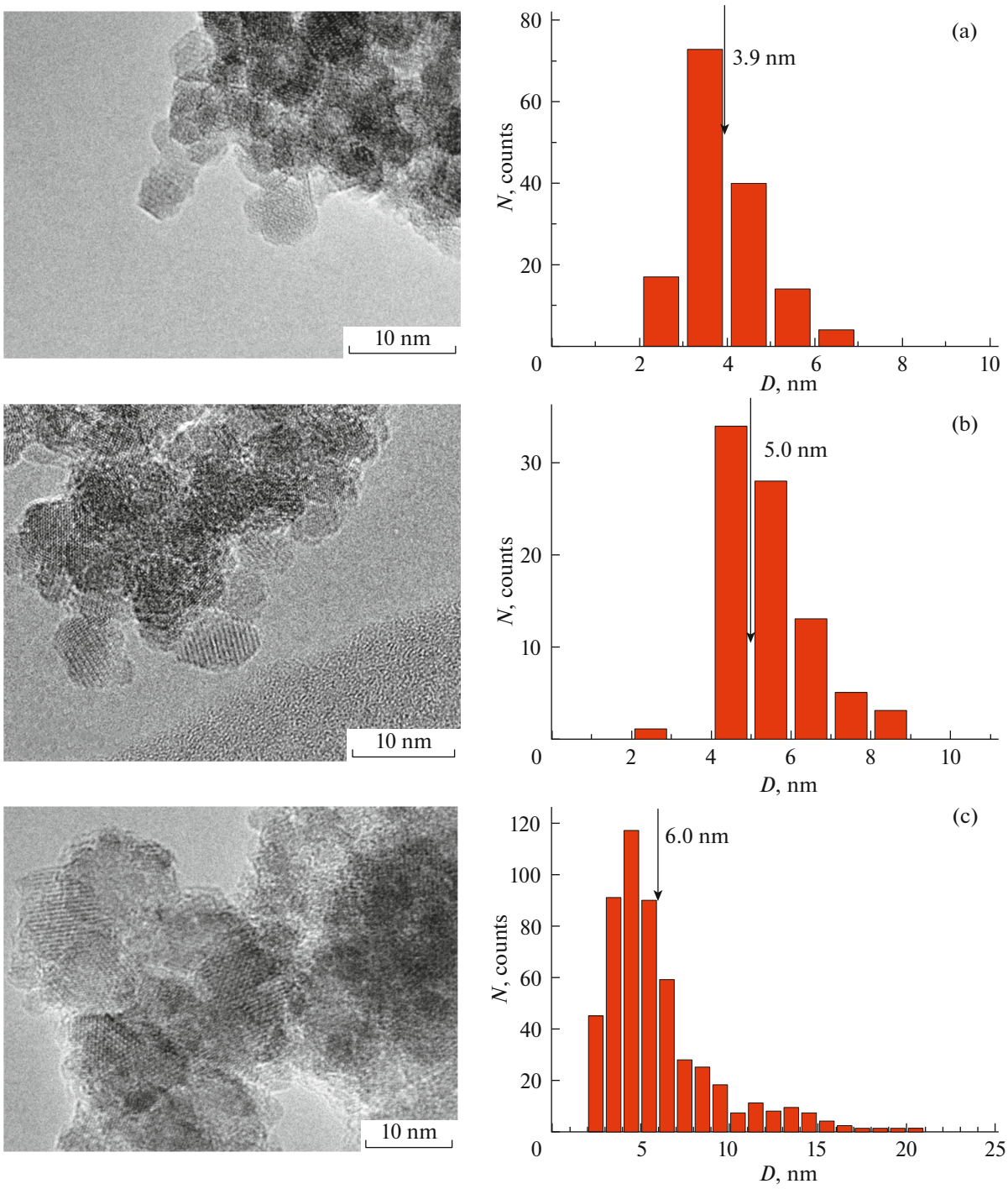

Fig. 1. Microphotographs and size distribution of particles for samples (a) *S*1, (b) *S*2, and (c) *S*3.

~4 nm. This is close to the Fe_3O_4 particle core size in sample *S*2. Therefore, if the magnetite particles in sample *S*2 formed a separate superparamagnetic subsystem (and the $CoFe_2O_4$ particles, correspondingly, formed the second subsystem), then this would be reflected in the temperature dependences of magnetization $M(T)_{ZFC}$ as an additional low-temperature maximum. The aforesaid was confirmed by the temperature dependences of magnetization $M(T)$ measured in fields of 100 and 500 Oe (Fig. 3). Thus, based on the analysis of the $M(T)$ dependences for the obtained samples, we can speak about the indirect confirmation of a core-shell particle structure ($Fe_3O_4/CoFe_2O_4$) in sample *S*2.

Figure 4 shows the magnetic hysteresis loops $M(H)$ of the investigated samples obtained at $T = 4.2$ K. The

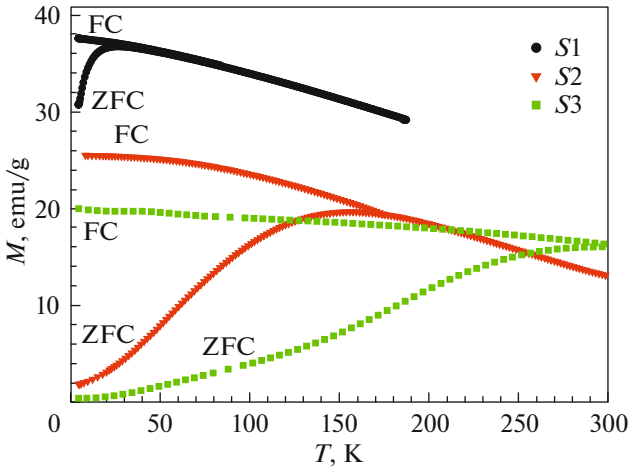

Fig. 2. Temperature dependences of magnetization for the samples in a field of $H = 1$ kOe in the ZFC and FC modes.

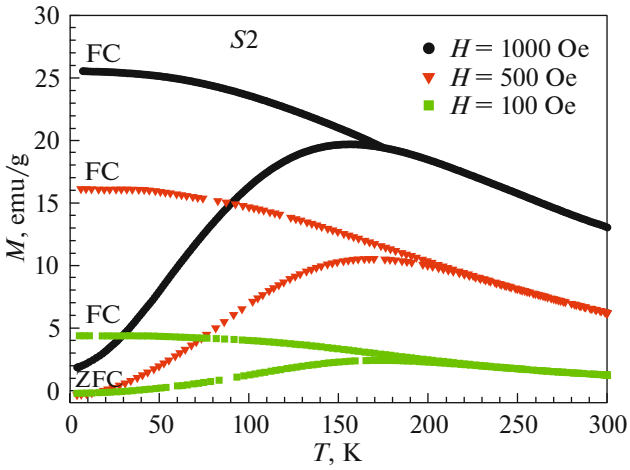

Fig. 3. Temperature dependences of magnetization for sample $S2$ ($Fe_3O_4/CoFe_2O_4$) in different external fields in the ZFC and FC modes.

coercivity H_C of soft magnetic material (magnetite) is relatively low ($H_C \sim 450$ Oe), which is typical of nanoparticles of such size [24, 30]. In samples $S2$ and $S3$, the H_C values are already ~12.65 and 9.2 kOe, respectively. It is reasonable to compare the temperature behaviors of the coercivity of these hard magnetic samples.

It is well-known that the temperature dependence $H_C(T)$ of the systems of single-domain ferro- and ferrimagnetic particles can be described by the expression [31, 32]

$$H_C(T) = H_C(T = 0)[1 - (T/T_B)^{0.5}], \quad (1)$$

where T_B is the superparamagnetic blocking temperature. Figure 5 shows the $H_C(T)$ dependences for samples $S2$ and $S3$ in the coordinates H_C, $T^{1/2}$. For sample $S3$, the points fit well a straight. The point of intersection of this straight with the abscissa axis is ~190 K at $H_C(T = 0) = 10.8$ kOe, which corresponds to the average blocking temperature $\langle T_B \rangle$ (see above). The deviation from dependence (1) at higher temperatures is caused by the effect of the coarsest particles (the tail of the distribution function) [33, 34].

In Fig. 5, one can also see that, for sample $S2$, the experimental points do not obey the linear dependence predicted by Eq. (1). The analysis of the $H_C(T)$ dependence showed that it can be approximated by the exponential dependence

$$H_C(T) = H_C(T = 0)\exp(-\beta T). \quad (2)$$

The inset in Fig. 5 shows the $H_C(T)$ dependence for sample $S2$ in semilogarithmic coordinates. The experimental points fit well a straight ($\beta = 0.029$ K^{-1} at $H_C(T = 0) = 13.5$ kOe), which confirms dependence (2). It is worth noting that the temperature dependence of the coercivity sharper than that predicted by conventional expression (1) was observed in the systems of ferrimagnetic nanoparticles [35–38]. The exponential $H_C(T)$ dependence of type (2) was obtained on the γ-Fe_2O_3 particles 10 nm in size [35] (the constant β in Eq. (2) = 0.02 K^{-1}), Fe_3O_4 particles 10 nm in size [36] (at $\beta = 0.014$–0.019 K^{-1}), and core-shell Fe_3O_4/γ-Fe_2O_3 particles 6–12 nm in size [37]. The authors of [36] and [35] explained well this extraordinary $H_C(T)$ dependence by the effect of magnetic interparticle interactions.

The effect of interparticle interactions on the properties of a system of magnetic nanoparticles is a fairly frequently met phenomenon [22], while the dependence of type (2) is extremely rare. In our case, at similar particle sizes and saturation magnetizations (Fig. 4) in samples $S2$ and $S3$, the interparticle inter-

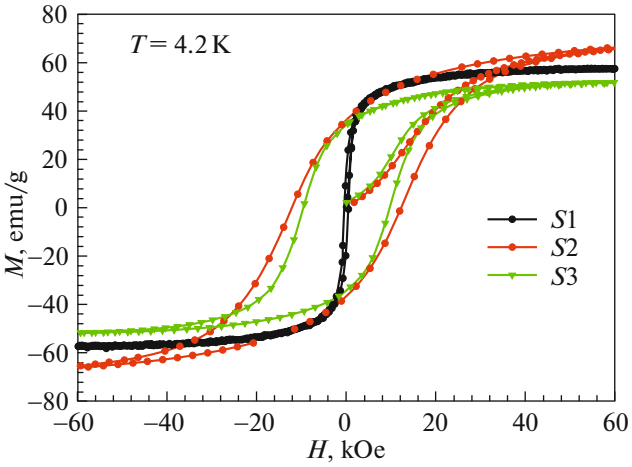

Fig. 4. Magnetic hysteresis loops of the samples at $T = 4.2$ K.

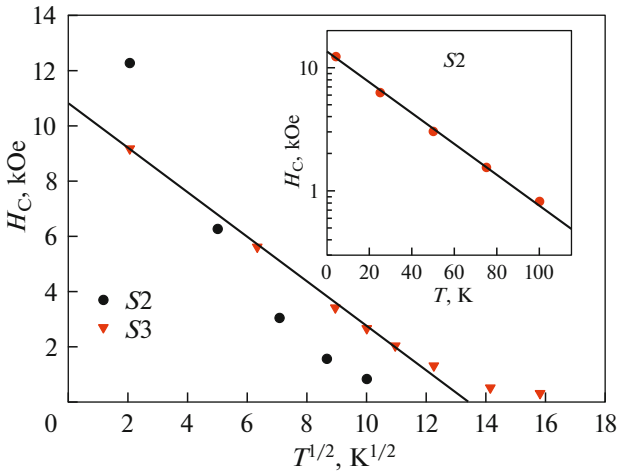

Fig. 5. Dependences of the coercivity H_C of samples *S*2 and *S*3 on $T^{1/2}$. Inset: $H_C(T)$ dependence for sample *S*2 in semilogarithmic coordinates. Solid lines are plotted using Eqs. (1) and (2) (see the text).

actions can be assumed similar. Therefore, it is reasonable to conclude that the observed difference in the temperature behaviors of $H_C(T)$ for these samples is caused by the difference between the structures of constituent particles. It can be assumed that the atypically fast drop coercivity with increasing temperature in sample *S*2 is caused by the temperature-dependent processes related to the interaction of the magnetic phases of the Fe_3O_4 core and $CoFe_2O_4$ shell inside a hybrid particle.

4. CONCLUSIONS

In this study, we proposed a new method for synthesizing core-shell nanoparticles and obtained the $Fe_3O_4/CoFe_2O_4$ system with a Fe_3O_4 core size of 2.5 nm and a $CoFe_2O_4$ shell size of 1.25 nm and a narrow particle size distribution. The investigations of the magnetic properties of the obtained hybrid particles and reference Fe_3O_4 and $CoFe_2O_4$ ones showed that the obtained $Fe_3O_4/CoFe_2O_4$ nanoparticles are, in fact, a core–shell system. In addition, we emphasized the atypical exponential (Eq. (2)) temperature dependence of the coercivity observed for the core–shell particles, which can be related to the features of the interaction between the magnetic phases of the core and shell.

The results obtained give grounds to use the developed method in synthesis and study of the highly dispersed oxide systems based on different size nanoparticles with a soft magnetic shell and a hard magnetic core and vice versa and seek for the effects related to the interaction of the core and shell magnetic phases.

FUNDING

This study was supported by the Russian Science Foundation, project no. 17-12-01111.

CONFLICT OF INTEREST

The authors declare that they have no conflicts of interest.

REFERENCES

1. A. K. Gupta and M. Gupta, Biomaterials **26**, 3995 (2005).
2. M. B. Gawande, P. S. Branco, and R. S. Varma, Chem. Soc. Rev. **42**, 3371 (2013).
3. T. Dang-Bao, D. Pla, I. Favier, and M. Gómez, Catalysts **7**, 207 (2017).
4. B. Thiesen and A. Jordan, Int. J. Hyperth. **24**, 467 (2008).
5. M.-H. Phan, J. Alonso, H. Khurshid, P. Lampen-Kelley, S. Chandra, K. Stojak Repa, Z. Nemati, R. Das, Ó. Iglesias, and H. Srikanth, Nanomaterials **6**, 221 (2016).
6. R. Skomski, J. Phys.: Condens. Matter **15**, R841 (2003).
7. S. S. Yakushkin, D. A. Balaev, A. A. Dubrovskiy, S. V. Semenov, Y. V. Knyazev, O. A. Bayukov, V. L. Kirillov, R. D. Ivantsov, I. S. Edelman, and O. N. Martyanov, Ceram. Int. **44**, 17852 (2018).
8. S. S. Yakushkin, A. A. Dubrovskiy, D. A. Balaev, K. A. Shaykhutdinov, G. A. Bukhtiyarova, and O. N. Martyanov, J. Appl. Phys. **111**, 44312 (2012).
9. S. L. Viñas, K. Simeonidis, Z.-A. Li, Z. Ma, E. Myrovali, A. Makridis, D. Sakellari, M. Angelakeris, U. Wiedwald, M. Spasova, and M. Farle, J. Magn. Magn. Mater. **415**, 20 (2016).
10. J.-H. Lee, J-t. Jang, J-s. Choi, S. H. Moon, S-h. Noh, J-w. Kim, J-G. Kim, I-S. Kim, K. I. Park, and J. Cheon, Nat. Nanotechnol. **6**, 418 (2011).
11. D. Psimadas, G. Baldi, C. Ravagli, M. Comes Franchini, E. Locatelli, C. Innocenti, C. Sangregorio, and G. Loudos, Nanotechnology **25**, 025101 (2014).
12. S. H. Moon, A.-H. Noh, J.-H. Lee, T.-H. Shin, Y. Lim, and J. Cheon, Nano Lett. **17**, 800 (2017).
13. A. S. Kamzin, I. M. Obaidat, A. A. Valliulin, V. G. Semenov, I. A. Al-Omari, and C. Nayek, Tech. Phys. Lett. **45**, 426 (2019).
14. A. S. Kamzin, A. A. Valiullin, H. Khurshid, Z. Nemati, H. Srikanth, and M. H. Phan, Phys. Solid State **60**, 382 (2018).
15. A. S. Kamzin, D. S. Nikam, and S. H. Pawar, Phys. Solid State **59**, 156 (2017).
16. J. Robles, R. Das, M. Glassell, M. H. Phan, and H. Srikanth, AIP Adv. **8**, 056719 (2018).
17. F. Fabris, E. Lima, Jr., C. Quinteros, L. Neser, M. Granada, M. Sirena, R. D. Zysler, H. E. Troiani, V. Leborán, F. Rivadulla, and E. L. Winkler, Phys. Rev. Appl. **11**, 054089 (2019).
18. D. S. Schmool, Nanosci. Nanotechnol. Lett. **3**, 515 (2011).

19. S. H. Moon, S. Noh, J.-H. Lee, T.-H. Shin, Y. Lim, and J. Cheon, Nano Lett. **17**, 800 (2017).
20. R. Mansell, T. Vemulkar, D. C. M. C. Petit, Y. Cheng, J. Murphy, M. S. Lesniak, and R. P. Cowburn, Sci. Rep. **7**, 4257 (2017).
21. Z. Nemati, H. Khurshid, J. Alonso, M. H. Phan, P. Mukherjee, and H. Srikanth, Nanotechnology **26**, 405705 (2015).
22. D. A. Balaev, S. V. Semenov, A. A. Dubrovskiy, S. S. Yakushkin, V. L. Kirillov, and O. N. Martyanov, J. Magn. Magn. Mater. **440**, 199 (2017).
23. V. L. Kirillov, S. S. Yakushkin, D. A. Balaev, A. A. Dubrovskiy, S. V. Semenov, Y. V. Knyazev, O. A. Bayukov, D. A. Velikanov, D. A. Yatsenko, and O. N. Martyanov, Mater. Chem. Phys. **225**, 292 (2019).
24. V. L. Kirillov, D. A. Balaev, S. V. Semenov, K. A. Shaikhutdinov, and O. N. Martyanov, Mater. Chem. Phys. **145**, 75 (2014).
25. A. D. Balaev, Yu. V. Boyarshinov, M. M. Karpenko, and B. P. Khrustalev, Prib. Tekh. Eksp., No. 3, 167 (1985).
26. J. C. Denardin, A. L. Brandl, M. Knobel, P. Panissod, A. B. Pakhomov, H. Liu, and X. X. Zhang, Phys. Rev. B **65**, 064422 (2002).
27. D. Tobia, E. Winkler, R. D. Zysler, M. Granada, H. E. Troiani, and D. Fiorani, J. Appl. Phys. **106**, 103920 (2009).
28. D. A. Balaev, A. A. Krasikov, A. A. Dubrovskiy, S. I. Popkov, S. V. Stolyar, O. A. Bayukov, R. S. Iskhakov, V. P. Ladygina, and R. N. Yaroslavtsev, J. Magn. Magn. Mater. **410**, 71 (2016).
29. D. A. Balaev, A. A. Krasikov, S. V. Stolyar, R. S. Iskhakov, V. P. Ladygina, R. N. Yaroslavtsev, O. A. Bayukov, A. M. Vorotynov, M. N. Volochaev, and A. A. Dubrovskii, Phys. Solid State **58**, 1782 (2016).
30. D. Caruntu, G. Caruntu, and C. J. O'Connor, J. Phys. D **40**, 5801 (2007).
31. L. Neel, Ann. Geophys. **5**, 99 (1949).
32. W. F. Brown, Phys. Rev. **130**, 1677 (1963).
33. S. V. Komogortsev, R. S. Iskhakov, A. D. Balaev, A. G. Kudashov, A. V. Okotrub, and S. I. Smirnov, Phys. Solid State **49**, 734 (2007).
34. S. V. Komogortsev, R. S. Iskhakov, A. D. Balaev, A. V. Okotrub, A. G. Kudashov, N. A. Momot, and S. I. Smirnov, Phys. Solid State **51**, 2286 (2009).
35. V. Sreeja and P. A. Joy, Mater. Res. Bull. **42**, 1570 (2007).
36. J. Lee, Y.-H. Choa, J. Kim, and K. H. Kim, IEEE Trans. Magn. **47**, 2874 (2011).
37. Y. Hwang, S. Angappane, J. Park, K. An, T. Hyeon, and J.-G. Park, Curr. Appl. Phys. **12**, 808 (2012).
38. A. P. Safronov, I. V. Beketov, S. V. Komogortsev, G. V. Kurlyandskaya, A. I. Medvedev, D. V. Leiman, A. Larrañaga, and S. M. Bhagat, AIP Adv. **3**, 052135 (2013).

Translated by E. Bondareva